crystals

MDPI

Article

Triple-Ringed Luminescent Heptanuclear Zn(II) Cluster for Efficient Ag(I) Ion Sensing Materials

Qian-Jun Deng [1,*], Min Chen [1], Dong-Chu Chen [1], Zhong-Hong Zhu [2,*] and Hua-Hong Zou [2,*]

[1] School of Material Science and Energy Engineering, Foshan University, Foshan 528000, China
[2] State Key Laboratory for Chemistry and Molecular Engineering of Medicinal Resources, School of Chemistry & Pharmacy of Guangxi Normal University, Guilin 541004, China
* Correspondence: dqj39@163.com (Q.-J.D.); 18317725515@163.com (Z.-H.Z.); zouhuahong@163.com (H.-H.Z.)

Received: 1 July 2019; Accepted: 17 July 2019; Published: 22 July 2019

Abstract: The organic ligands (*E*)-8-hydroxyquinoline-2-carbaldehyde oxime (H_2L^1) and furan-2-ylmethanamine (H_2L^2) were used to react with $Zn(NO_3)_2{\cdot}6H_2O$ at 140 °C solvothermal for two days to obtain the heptanuclear Zn(II) cluster $[Zn_7(L^1)_4(HL^1)_2(H_2L^2)(\mu_2\text{-OH})(\mu_2\text{-O})(NO_3)]$ (**1**). The X-ray single crystal diffraction reveals that every five-coordinated Zn(II) ions are surrounded by two N atoms and three O atoms with the N_2O_3 coordination environment and four-coordinated Zn(II) ion surrounded by one N atom and three O atoms in the NO_3 coordinated environment. The photoluminescence of cluster **1** is obvious. Moreover, in the presence of Ag(I) ions, cluster **1** exhibits an efficient recognition ability, and it realizes the recognition of toxic metal ions. Here, we have developed cluster-based sensing materials for the efficient detection of heavy metal ions Ag(I) strategies.

Keywords: luminescent; heptanuclear Zn(II) cluster; Ag(I) ion detection; sensing materials

1. Introduction

Silver-containing materials are widely used in industrial production and medicine, they have been widely used as catalysts [1], electrodes [2], and antimicrobial agents [3]. However, during such frequent use of silver-containing materials, more and more attention has been paid to the harmful effects of silver ions on human health and the environment [4,5]. Therefore, it is very important to establish effective silver ion detection methods for drinking water, food, and ecological safety [6]. Although there are other methods for silver determination, atomic absorption spectrometry and inductively coupled plasma atomic emission spectrometry or mass spectrometry are generally used [7–11]. However, these detection methods have the disadvantage of being a complex process, requiring expensive instruments, and are time-consuming. In order to solve these deficiencies, scientists have made tremendous efforts and devoted themselves to explore simple and efficient methods, such as colorimetry and fluorimetry.

In the past decades, various complex organic molecular probes have been reported for the detection of silver ions [12]. However, the synthesis of these organic probes is complicated. Some easy-to-prepare nanomaterials have also been developed for the detection of silver ions, and have become another hot topic [13–15]. However, there are very few examples of silver ion detection compared with these complexes. The complex detection of metal ions may lead to the substitution of the detected metal ions with the coordination metal due to the unstable structure of the complex, which further changes the spectral properties of the metal ions and realizes the effective detection of heavy metal ions [16–18]. Therefore, it is necessary to establish a set of effective detection methods, which can selectively identify different metal ions by complexes, so as to provide development opportunities for the detection of specific heavy metal ions.

Herein, we obtained a heptanuclear Zn(II) cluster $[Zn_7(L^1)_4(HL^1)_2(H_2L^2)(\mu_2\text{-OH})(\mu_2\text{-O})(NO_3)]$ (**1**) upon treating with (*E*)-8-hydroxyquinoline-2-carbaldehyde oxime (H_2L^1), furan-2-ylmethanamine (H_2L^2) and $Zn(NO_3)_2{\cdot}6H_2O$ at 140 °C for two days with CH_3CN. Cluster **1** contains three different coordinated Zn(II) ions, which result from the various coordinating modes of organic ligands, and the weak supramolecular actions make the structure stack into a three-dimensional framework. The fluorescence data suggest that cluster **1** is an obvious photoluminescent material. Further, we tested the sensitivity of cluster **1** for sensing materials for the detection of heavy metal ions. The detection results of ten different types of metal ions by cluster **1** show that when Ag(I) ions are added to the *N*,*N*-dimethylformamide (DMF) solution containing **1**, the luminescence intensity of the system increases rapidly. It was found that cluster **1** could effectively identify Ag(I) ions, and it also has certain recognition ability to some rare-earth ions.

2. Results and Discussion

Crystal Structure. The X-ray single crystal diffraction suggests that complex **1** crystallizes in the monoclinic crystal system with the space group $P2_1/c$ (Table 1), in which five-coordinated Zn(II) ions (Zn1 and Zn2) are surrounded by two N atoms from one ligand and three O atoms from three ligands within the N_2O_3 coordination environment. Another five-coordinated Zn(II) ions (Zn3, Zn4, Zn5, and Zn6) are surrounded by two N atoms from one ligand, three O atoms from two ligands, and one μ_2-O ion within the N_2O_3 coordinated environment, and four-coordinated Zn(II) ion (Zn7) is surrounded by one N atom from one furan-2-ylmethanamine ligand (HL^2), two O ions from two ligands, and one oxygen atom from the nitrate anion with the NO_3 coordination environment (Figure 1a), so its molecular formula is $[Zn_7(L^1)_4(HL^1)_2(H_2L^2)(\mu_2\text{-OH})(\mu_2\text{-O})(NO_3)]$. By using *SHAPE*, software the calculated result suggests that the five-coordinative Zn^{II} could be viewed as a trigonal bipyramidal configuration, a spherical square pyramidal configuration, and the four-coordinative Zn(II) could be viewed as a spherical, square pyramidal configuration (Table S2). The bond length distances between Zn(II) ion and ligand nitrogen atoms fall into the range of 1.962–2.420 Å, the bond length distances between Zn(II) ion and ligand oxygen atoms fall into the range of 1.900–2.206 Å, the bond distances of Zn-O fall in the range of 1.915–1.964 Å between Zn(II) ion and the oxygen ions of μ_2-O^{2-} or μ_2-OH, the bond distance of Zn-N between Zn(II) ion and H_2L^2 ligand is 2.033 Å, and the bond distance of Zn-O is 1.987 Å between Zn(II) ion and nitrate anion (Table S1). The molecular supramolecular weak action of **1** contains three type of interactionss, which are C−H···O hydrogen bond (Figure 1b), C-H···π weak interaction (Figure 1c), and π···π weak interactions (Figure 1d). The above-mentioned supramolecular weak action distances were all within a reasonable range, and the supramolecular weak actions make the structure stack into a three-dimensional network (Figure 2) [19]. Therefore, it could be considered as a formation of 5-connected ***shp*** nets (Figure 2) with distances of 10.052–14.177 Å [20]. The thermogravimetric analysis (TGA) was carried out to examine the thermal stability of complex **1**. The sample was heated up to 800 °C in N_2 at a heating rate of 5 °C/min. The first weight loss (8.63%) experienced by **1** over the temperature range of 30 °C to 200 °C corresponds to the release of one coordinative nitrate anion and one H_2L^2 ligand (calculated, 9.52%) (Figure S1 in Supplementary Materials)

Table 1. Crystallographic data of the complex **1**.

Complex	**1**
Formula	$C_{65}H_{46}N_{14}O_{18}Zn_7$
Formula weight	1768.75
T (K)	293.15
Crystal system	Monoclinic
Space group	$P2_1/c$
a (Å)	10.8123(4)
b (Å)	18.0040(8)
c (Å)	34.376(3)

Table 1. *Cont.*

Complex	1
α (°)	90.00
β (°)	95.493(4)
γ (°)	90.00
V (Å^3)	6661.1(6)
Z	4
D_c (g cm^{-3})	1.764
μ (mm^{-1})	2.561
Reflns coll.	38035
Unique reflns	12360
R_{int}	0.1095
$^aR_1$ [$I \geq 2\sigma(I)$]	0.0879
$^bwR_2$ (all data)	0.2473
GOF	1.047

$^aR_1 = \Sigma||F_o|-|F_c||/\Sigma|F_o|$, $^bwR_2 = [\Sigma w(F_o^2-F_c^2)^2/\Sigma w(F_o^2)^2]^{1/2}$.

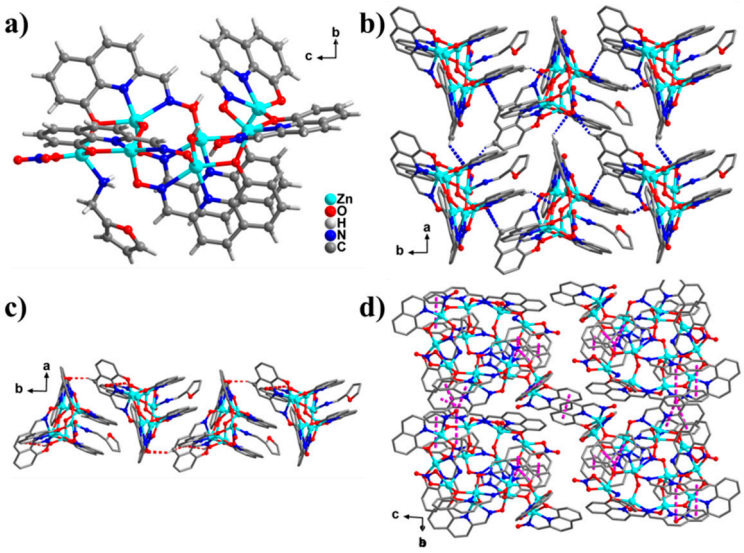

Figure 1. (**a**) The structure of complex **1**; (**b**) the C-H···O weak interactions (blue dotted lines); (**c**) the C-H···π weak interactions (red dotted lines); (**d**) the π···π weak interactions (pink dotted lines).

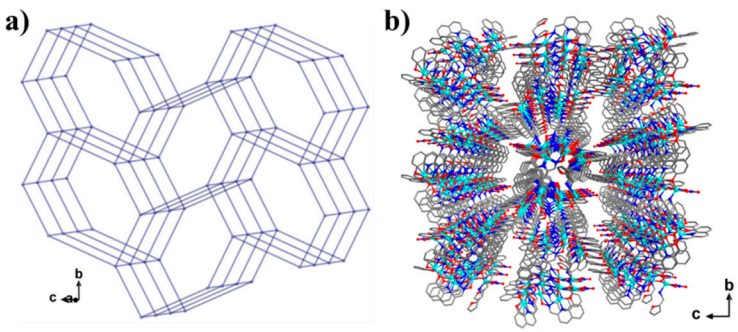

Figure 2. (**a**) The connecting modes of the clusters through the C–H···π, π···π interactions and hydrogen bonds in complex **1**; (**b**) and its stacking mode.

The electronic configuration of the Zn(II) ion allows Zn(II) clusters to have a photoluminescence effect when they chelate with planar conjugated ligands to form complexes. The photophysical properties of complex **1** were determined by UV-Vis spectroscopy in a DMF solution containing

1 mg/mL concentration (Figure S2). We occasionally found that the complex dissolved in DMF had strong luminescence under an ultraviolet lamp. Therefore, we suspect that cluster **1** is likely to be used to identify different metal ions. Ultraviolet measurements showed that the heavy metal ions had obvious ultraviolet absorption at 266 nm after they were added into the complex solution. For Cr(II) ions, low-intensity acromion appeared at 472 and 648 nm.

Based on the above results, we try to detect and identify some toxic heavy metal ions. Therefore, we choose Cr(II), Mn(II), Fe(II), Ni(II), Cu(II), Cd(II), Ag(I), Dy(III), Gd(III), and Tm(III) metal salts, 10 μg/mL concentration of DMF solution. The sample of 20 mg complex **1** is dissolved in 40 mL DMF, and the solution of complex **1** is divided into 10 phr, that is, 2 mL of 1 mg/mL complex solution is to be used. The prepared metal salt solution of 1 mL was added into the solution of complex **1** and mixed uniformly. The photophysical properties of complex **1** mixed with metal ions were determined by UV-vis spectrum and fluorescence spectroscopy, respectively. As shown in Figure 3, complex **1** exhibits the metal ion specificity of fluorescence response at 547 nm under the excitation of 266 nm wavelength, in which the fluorescence enhancement is obviously Ag^+ specific. Dy(III) and Gd(III) can induce smaller fluorescence enhancement at this wavelength, and Cr(II), Mn(II), Fe(II), Ni(II), Cu(II), Cd(II), and Tm(III) at this wavelength cause smaller fluorescence enhancement. For all metal salts, the fluorescence enhancement at 547 nm wavelength could be attributed to ligand luminescence. When complex **1** solution is mixed with Dy(III) metal salt, the fluorescence tests show that there is another peak at 547 nm. We suspect that there are possible coordination sites in the HL^1 and H_2L^2 ligands, which can bind to Dy(III) ions, resulting in the occurrence of a subsequent set of peaks. We analyzed the highly selective detection of Ag(I) ions in complex **1**. It was found that, because of the similar electronic configuration between Ag(I) and Zn(II) ions, the exchange of Zn→Ag between Ag(I) and some Zn(II) ions in the structure occurred, and the coordination with ligands occurred. After the exchange, the luminescence of the solution was very strong, and the metal-ligand charge transfer (MLCT) occurred effectively. Moreover, Zn(II) and Ag(I) had a similar peripheral electron arrangement, showing a preference for homologous metal ions.

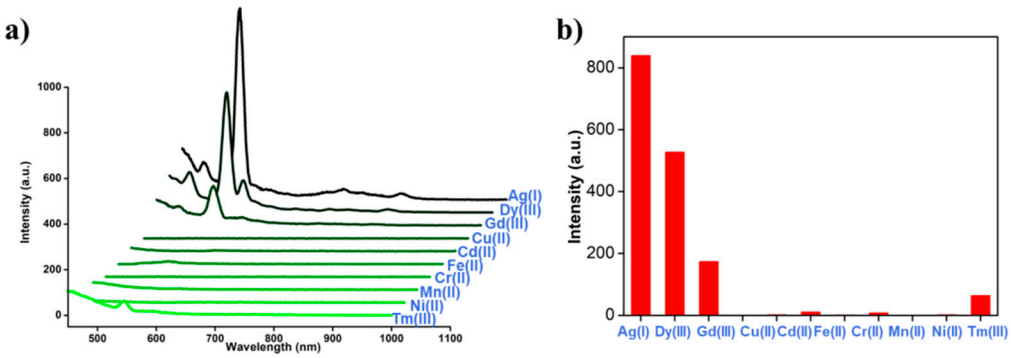

Figure 3. (**a**) Fluorescence spectral changes for complex **1**; (**b**) the relative fluorescence intensity at 547 nm in the presence of 1 equivalent of metal ions in DMF at 25 °C.

3. Conclusions

In summary, we used (*E*)-8-hydroxyquinoline-2-carbaldehyde oxime, furan-2-ylmethanamine to coordinate with Zn(II) ions under solvothermal conditions to obtain a heptanuclear Zn(II) complex. Six Zn(II) ions are coordinated with an N_2O_3 coordinative environment, and one Zn(II) ion is four coordination with NO_3 coordinative environment. The weak interactions analysis shows that every Zn_7 structure is connected to form a 3D framework. The luminescence study suggests that complex **1** is an obvious photoluminescent material, and complex **1** has high selective recognition ability for toxic heavy metal Ag(I) ions. This provides a simple and new method for the efficient detection of heavy metal ions by cluster-based sensing materials.

4. Experimental

4.1. Materials and Measurements

All reagents were obtained from commercial sources and used without further purification. Elemental analyses for C, H, and N were performed on a Vario Micro Cube. Thermogravimetric analyses (TGA, NETZSCH, Selb, Germany) were performed in a flow of nitrogen at a heating rate of 10 °C/min using a NETZSCH TG 209 F3 (Figure S1). Infrared spectra were recorded by transmission through KBr pellets containing ca. 0.5% of the complexes using a PE Spectrum FT-IR spectrometer (400–4000 cm^{-1}, Gangdong, Tianjin, China).

4.2. Single-Crystal X-ray Crystallography

Diffraction data for these complexes were collected on a Bruker SMART CCD diffractometer (Mo Kα radiation and λ = 0.71073 Å) in Φ and ω scan modes. The structures were solved by direct methods followed by difference Fourier syntheses and then refined by full-matrix least-squares techniques on F^2 using SHELXL [21]. All other non-hydrogen atoms were refined with anisotropic thermal parameters. Hydrogen atoms were placed at calculated positions and refined isotropically using a riding model. The number of free solvent molecules has been further confirmed by elemental analyses and TGA analysis (Figure S1). X-ray crystallographic data and refinement details for the complexes are summarized in Table S1. Full details are found in the crystallgraphic information files (CIF) files provided in the Supporting Information. The CCDC reference numbers are 1934766.

*4.3. Synthesis of Complex **1***

A total of 0.0475 g (0.25 mmol) of (*E*)-8-hydroxyquinoline-2-carbaldehyde oxime (H_2L^1) was weighed and four drops furan-2-ylmethanamine (H_2L^2) were added to 15 mL CH_3CN, then 0.0745 g (0.25 mmol) $Zn(NO_3)_2{\cdot}6H_2O$ was added, and the solution stired for 5 minutes with a magnetic stirrer (Synthware, Beijing, China) at room temperature, and then transferred to a Teflon reactor (Synthware, Beijing, China) with a volume of 25 mL, placed directly in an oven (Marit, Wuxi, China) at 80 °C for 24 hours, then cooled at room temperature. The complex was then washed with fresh CH_3CN solvent which gave a red strip of clear crystals with a yield of about 57% based on $Zn(NO_3)_2{\cdot}6H_2O$. The main infrared spectrum data of complex **1** were (KBr, cm^{-1}): 3470 (s), 1522 (m), 1501 (s), 1338 (m), 1264 (m), 1106 (s), 826 (m), 752 (m). The elemental analysis (%) ($C_{65}H_{46}N_{14}O_{18}Zn_7$): Calculated: C, 44.13; H, 2.62; N, 11.09; Found: C, 43.86; H, 2.48; N, 10.85.

Supplementary Materials: The following are available online at http://www.mdpi.com/2073-4352/9/7/374/s1, Figure S1: The scheme with the structures of H_2L^1 and H_2L^2, Figure S2: The coordination pattern diagram of Zn(II) ions in compound **1**, Figure S3: Thermogravimetry of the compounds at a heating rate of 5 °C/min under N_2 atmosphere for **1**, Figure S4: The UV-visible absorption spectrum of the ligand H$\mathbf{L^1}$ and compound **1** dissolved in DMF, respectively, Figure S5: Fluorescence spectra of ligand H$\mathbf{L^1}$ (a) and compound **1** (b) dissolved in DMF, respectively, Figure S6: The complex **1** and different metal ions were dissolved in an ultraviolet-visible absorption test in DMF, Table S1: Selected bond lengths (Å) and angles (°) of **1**, Table S2: *SHAPE* analysis in complex **1**.

Author Contributions: Conceptualization, H.-H.Z and Z.-H.Z.; methodology, Q.-J.D.; software, M.C.; validation, Q.-J.D, Z.-H.Z, and H.-H.Z.; formal analysis, Q.-J.D.; investigation, D.-C.C.; resources, Q.-J.D.; data curation, M.C.; writing—original draft preparation, Z.-H.Z.; writing—review and editing, H.-H.Z.; visualization, Q.-J.D.; supervision, D.-C.C.; project administration, Q.-J.D.; funding acquisition, Q.-J.D.

Funding: This research was funded by the Nature Science Foundation of China (No. 51872047 and 21601038), the key Project of Department of Education of Guangdong Province (2016GCZX008), the Science and Technique Innovation Foundation of Foshan City (2017AB004041), Guangxi Natural Science Foundation (2016GXNSFAA380085).

Acknowledgments: This work was supported by the Nature Science Foundation of China (No. 51872047 and 21601038), the key Project of Department of Education of Guangdong Province (2016GCZX008), the Science and Technique Innovation Foundation of Foshan City (2017AB004041), Guangxi Natural Science Foundation (2016GXNSFAA380085).

Conflicts of Interest: The authors declare no conflict of interest.

References

1. Lu, J.; Bravo-Suárez, J.J.; Takahashi, A.; Haruta, M.; Oyama, S.T.J. In situ UV–vis studies of the effect of particle size on the epoxidation of ethylene and propylene on supported silver catalysts with molecular oxygen. *J. Catal.* **2005**, *232*, 85–95. [CrossRef]
2. Wu, H.; Kong, D.; Ruan, Z.; Hsu, P.; Wang, S.; Yu, Z.; Carney, T.J.; Hu, L.; Fan, S.; Cui, Y. A transparent electrode based on a metal nanotrough network. *Nat. Nanotechnol.* **2013**, *8*, 421–425. [CrossRef] [PubMed]
3. Chernousova, S.; Epple, M. Silver as Antibacterial Agent: Ion, Nanoparticle, and Metal. *Angew. Chem. Int. Ed.* **2013**, *52*, 1636–1653. [CrossRef] [PubMed]
4. Barriada, J.L.; Tappin, A.D.; Evans, E.H.; Achterberg, E.P. Dissolved silver measurements in seawater. *Trends Anal. Chem.* **2007**, *26*, 809–817. [CrossRef]
5. Bian, L.; Ji, X.; Hu, W.J. A Novel Single-Labeled Fluorescent Oligonucleotide Probe for Silver(I) Ion Detection in Water, Drugs, and Food. *Agric. Food Chem.* **2014**, *62*, 4870–4877. [CrossRef]
6. Lai, C.Z.; Fierke, M.A.; Costa, R.C.; Gladysz, J.A.; Stein, A.; Bühlmann, P. Highly Selective Detection of Silver in the Low ppt Range with Ion-Selective Electrodes Based on Ionophore-Doped Fluorous Membranes. *Anal. Chem.* **2010**, *82*, 7634–7640. [CrossRef] [PubMed]
7. Sanchez-Pomales, G.; Mudalige, T.; Lim, J.; Linder, S.W.J. Rapid Determination of Silver in Nanobased Liquid Dietary Supplements Using. *Agric. Food Chem.* **2013**, *61*, 7250–7257. [CrossRef]
8. Yang, H.; Liu, X.; Fei, R.; Hu, Y. Sensitive and selective detection of Ag^+ in aqueous solutions using Fe_3O_4@Au nanoparticles as smart electrochemical nanosensors. *Talanta* **2013**, *116*, 548–553. [CrossRef]
9. Bian, S.; Shen, C.; Qian, Y.; Liu, J.; Xi, F.; Dong, X. Facile synthesis of sulfur-doped graphene quantum dots as fluorescent sensing probes for Ag^+ ions detection. *Sens. Actuators B Chem.* **2017**, *242*, 231–237. [CrossRef]
10. Batista, B.L.; da Silva, L.R.S.; Rocha, B.A.; Rodrigues, J.L.; Berretta-Silva, A.A.; Bonates, T.O.; Gomes, V.S.D.; Barbosa, R.M.; Barbosa, F. Multi-element determination in Brazilian honey samples by inductively coupled plasma mass spectrometry and estimation of geographic origin with data mining techniques. *Food Res. Int.* **2012**, *49*, 209–215. [CrossRef]
11. Song, Q.J.; Greenway, G.M.; McCreedy, T. Interfacing microchip capillary electrophoresis with inductively coupled plasma mass spectrometry for chromium speciation. *J. Anal. At. Spectrom.* **2003**, *18*, 1–3. [CrossRef]
12. Zheng, L.; Chi, Y.; Dong, Y.; Lin, J.; Wang, B. Electrochemiluminescence of Water-Soluble Carbon Nanocrystals Released Electrochemically from Graphite. *J. Am. Chem. Soc.* **2009**, *131*, 4564–4565. [CrossRef] [PubMed]
13. Jin, J.C.; Wang, B.B.; Xu, Z.Q.; He, X.H.; Zou, H.F.; Yang, Q.Q.; Jiang, F.L.; Liu, Y. A novel method for the detection of silver ions with carbon dots: Excellent selectivity, fast response, low detection limit and good applicability. *Sens. Actuators B Chem.* **2018**, *267*, 627–635. [CrossRef]
14. Gao, X.; Lu, Y.; Zhang, R.; He, S.; Ju, J.; Liu, M.; Li, L.; Chen, W. One-pot synthesis of carbon nanodots for fluorescence turn-on detection of Ag^+ based on the Ag^+-induced enhancement of fluorescence. *J. Mater. Chem. C* **2015**, *3*, 2302–2309. [CrossRef]
15. Ran, X.; Sun, H.; Pu, F.; Ren, J.; Qu, X. Ag Nanoparticle-decorated graphene quantum dots for label-free, rapid and sensitive detection of Ag^+ and biothiols. *Chem. Commun.* **2013**, *49*, 1079–1081. [CrossRef] [PubMed]
16. Hao, J.N.; Yan, B. A water-stable lanthanide-functionalized MOF as a highly selective and sensitive fluorescent probe for Cd^{2+}. *Chem. Commun.* **2015**, *51*, 7737–7740. [CrossRef]
17. Pandey, S.; Kumar, P.; Gupta, R. Polymerization led selective detection and removal of Zn^{2+} and Cd^{2+} ions: isolation of Zn- and Cd-MOFs and reversibility studies. *Dalton Trans.* **2018**, *47*, 14686–14695. [CrossRef]
18. Liao, W.M.; Wei, M.J.; Mo, J.T.; Fu, P.Y.; Fan, Y.N.; Pan, M.; Su, C.Y. Acidity and Cd^{2+} fluorescent sensing and selective CO_2 adsorption by a water-stable Eu-MOF. *Dalton Trans.* **2019**, *48*, 4489–4494. [CrossRef]
19. Zhu, Z.H.; Ma, X.F.; Wang, H.L.; Zou, H.H.; Mo, K.Q.; Zhang, Y.Q.; Yang, Q.Z.; Li, B.; Liang, F.P. A triangular Dy_3 single-molecule toroic with high inversion energy barrier: magnetic properties and multiple-step assembly mechanism. *Inorg. Chem. Front.* **2018**, *5*, 3155–3162. [CrossRef]

20. Benelli, C.; Gatteschi, D. Magnetism of Lanthanides in Molecular Materials with Transition-Metal Ions and Organic Radicals. *Chem. Rev.* **2002**, *102*, 2369–2387. [CrossRef]
21. Sheldrick, G.M. Crystal structure refinement with SHELXL. *Sect. C Struct. Chem.* **2015**, *71*, 3–8. [CrossRef] [PubMed]